Nanosecond Pulse Generation in Lumped Normally Dispersive All-Fiber Mode-Locked Laser

M. Zhang, E. J. R. Kelleher, E. D. Obraztsova, S. V. Popov, and J. R. Taylor

***Abstract*—We report an all-normal dispersion, all-fiber integrated ytterbium laser mode-locked by a single wall carbon nanotube (SWNT) saturable absorber, with a chirped fiber Bragg grating (CFBG) providing dispersion of 35.71 ps $\cdot$ nm^{-1} allowing us to directly obtain nanosecond-scale duration pulses. In this large positive dispersion regime, mode-locking is initiated by the saturable action of the SWNT device, with pulse formation stabilized by the combined bandwidth limiting effect of the gain dispersion and the narrow reflection band of the CFBG.**

***Index Terms*—Bragg gratings, fiber lasers, laser mode locking, ytterbium.**

I. Introduction

PASSIVELY mode-locked fiber laser sources, using saturable absorber devices, are now an accepted technology and are widely deployed in a broad range of applications requiring ultrashort pulses because of their compactness, stability, and low cost. Management of the cavity dispersion has permitted the development of robust high-power systems. Recently, passively mode-locked fiber lasers with an all-normal dispersion (ANDi) map were proposed to overcome the limits imposed by operating in the soliton regime [1], allowing the extraction of pulses with energies of hundreds of nanojoules [2]–[5]. Initiation of a regular pulse train from noise and pulse stabilization in ANDi mode-locked fiber lasers relies on the intensity dependent loss provided by the nonlinear action of a saturable absorber in combination with a bandwidth limited gain preventing pulse spreading. Such a pulse solution is known as a dissipative soliton [6], typically possessing a predominantly linear chirp suitable for compression to the femtosecond regime [7].

The generation of highly chirped nanosecond pulses directly in a normally dispersive oscillator was demonstrated by Kelleher *et al.*, utilizing a long length (1.2 km) of normally dispersive passive fiber providing a distributed dispersion to chirp the pulses on successive round-trips of the cavity, leading to the steady-state formation of highly-linearly chirped pulses [8]. It was also shown that the pulse duration was proportional to the length of passive fiber, with durations from tens of picoseconds to nanoseconds achievable for lengths from 20 m to 1.2 km. The long, kilometer length, dispersive fiber in the cavity lowers the fundamental repetition rate of the laser to the 100's kHz; such repetition rates often are not desirable in certain applications. In the previous work, attempts to produce stable mode-locked pulses with a lumped rather than distributed dispersion were unsuccessful, and it was concluded that the additional nonlinearity, through the action of self-phase modulation, provided by the long passive fiber, forming the distributed dispersion element, was necessary to generate the required spectral bandwidth to facilitate stable, steady-state nanosecond pulse mode-locked operation. Here we show that nanosecond pulses can be generated in a mode-locked cavity where the long passive dispersive fiber is substituted with an equivalent lumped dispersion element, but without additional nonlinearity. This demonstrates an additional advantage of producing desired pulse durations from shorter cavity lengths, permitting generation of nanosecond pulses at much faster MHz repetition rates. This result is also of interest from a fundamental dynamics perspective because it confirms that long pulse formation in a highly normally dispersive mode-locked cavity is affected mostly by linear dispersion rather than nonlinearity of the fiber. We provide results of numerical simulations which support the experimental realization of stable mode-locked operation using a purely lumped normal dispersion to generate nanosecond pulses from an all-fiber oscillator with a 6.6 MHz repetition frequency.

II. Experiment Setup

The configuration of the all-fiber laser is shown in Fig. 1. An ytterbium doped fiber amplifier module (IPG Photonics) was used to provide a noise seed and amplification in a band around 1.06 μm. A polarization independent in-line fiber circulator was used to incorporate the chirped Bragg grating, providing a normal dispersion of 35.71 ps $\cdot$ nm^{-1}, and ensured unidirectional propagation. Intensity dependent loss, to initiate mode-locking, was achieved by using a transparent carboxymetylcellulose film with homogeneously embedded individual SWNTs [9] synthesized by an arc-discharge technique [10]. The SWNT-based saturable absorber device had a modulation depth of $\sim$ 10% at 1.06 μm [11] corresponding to the second semiconductor electronic transition (S_2) in the density of states.

Manuscript received February 25, 2011; revised May 16, 2011; accepted June 24, 2011. Date of publication July 12, 2011; date of current version September 09, 2011. The Femtosecond Optics Group was supported by studentships from the U.K. Engineering and Physical Sciences Research Council and by the Royal Society. The work of M. Zhang was supported by China-UK Scholarships for Excellence. The work of J. R. Taylor was supported by a Royal Society Wolfson Research Merit Award.

M. Zhang, E. J. R. Kelleher, S. V. Popov, and J. R. Taylor are with the Femtosecond Optics Group, Department of Physics, Imperial College London, London, SW7 2AZ, U.K. (e-mail: m.zhang10@imperial.ac.uk).

E. D. Obraztsova is with the A.M. Prokhorov General Physics Institute, 119991, Moscow, Russia.

Color versions of one or more of the figures in this letter are available online at http://ieeexplore.ieee.org.

Digital Object Identifier 10.1109/LPT.2011.2161462

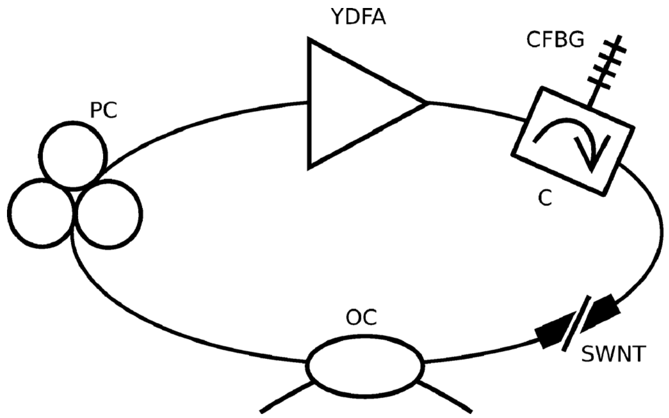

Fig. 1. Schematic of the fiber laser cavity: YDFA: ytterbium-doped fiber amplifier; C: circulator; CFBG: chirped fiber Bragg grating; SWNT: single wall carbon nanotubes; OC: output coupler; PC: polarization controller.

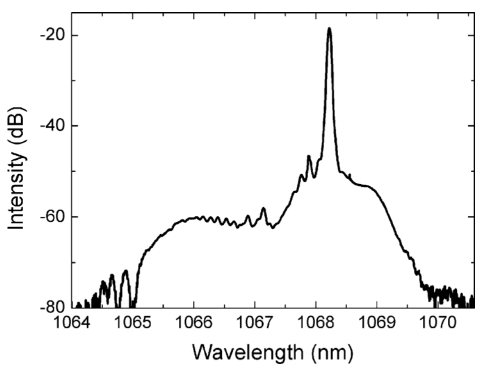

Fig. 2. Measured optical spectrum.

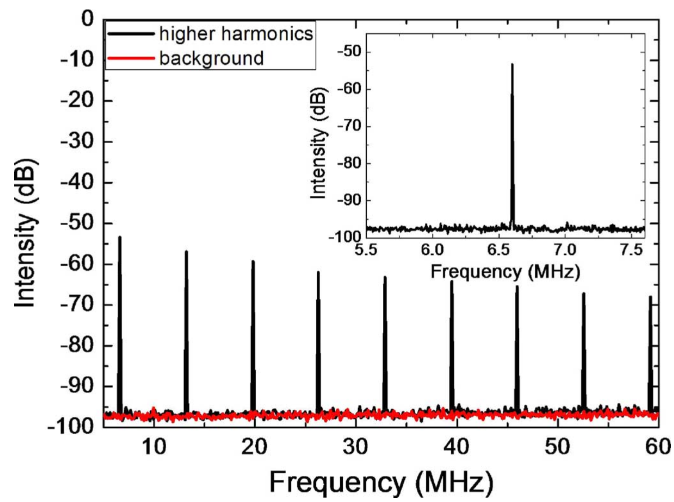

Fig. 3. Radio-frequency spectrum showing the cavity harmonics (red trace shows the noise floor of the device) and inset the fundamental harmonic on a 2-MHz span.

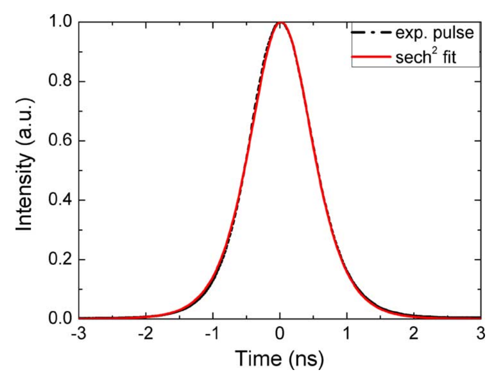

Fig. 4. Experimentally measured temporal intensity profile, with a sech^2 fit.

A polarization controller was added to adjust the polarization state within the cavity to optimize long-term operation, but was not fundamental to the mode-locking action. The output was delivered through a 20% fused-fiber coupler to both spectral (Ando optical spectrum analyzer) and temporal diagnostics (50 GHz Tektronix sampling scope and a photo-diode with a 15 ps rise-time).

III. Experiment Results and Discussion

Mode locking was obtained at the fundamental repetition frequency of the cavity of 6.6 MHz, with a corresponding single pulse energy of 15 pJ. The spectrum, centered at 1068.2 nm, is plotted in Fig. 2, with a full width at half maximum (FWHM) of 0.059 nm corresponding to a transform limited pulse duration of 20 ps, resulting in a time-bandwidth product of 18 indicating that the generated pulses are strongly chirped.

The contrast ratio between the lasing peak and the amplified spontaneous emission (ASE) background is $\sim$ 30 dB, limited by ASE generated because the laser operation wavelength, defined by the pass-band of the CFBG, did not overlap with the peak of the amplifier's gain. Fig. 3 shows higher cavity harmonics without any noticeable beat frequency shift, which would normally indicate longer-term instabilities. The mode-locked pulse width was 1.15 ns. The pulse temporal profile is plotted in Fig. 4 fitted with a sech^2 pulse shape. This is the expected pulse shape for a dissipative soliton as predicted by theory initially developed by Haus *et al.* and later by Renninger *et al.* [6], [12].

The mode-locking performance was dependent on the action of the SWNT saturable absorber and the filtering effect of the CFBG, with the pulse duration defined by the large lumped normal dispersion of the CFBG. Pulses broadened to a nanosecond by a long length of passive fiber were reported to possess a predominantly linear chirp [7]. However, because of the large time-bandwidth product compression is impractical with standard schemes, such as bulk gratings. As an example for an input pulse with a spectrum equal to our measured spectrum (0.059 nm), but a temporal duration two orders of magnitude shorter (11.5 ps) the required grating separation for a pair of bulk compression gratings with 1200 lines/mm and an incident angle of 45 degrees would be 31 m. As the separation scales linearly with the duration we would need over 3 km's separation to compensate a nanosecond pulse, assuming a linear chirp.

Numerical simulations of the laser system were carried out by solving a modified nonlinear Schrödinger equation, excluding higher order dispersion, shock formation and Raman terms. The CFBG was modeled by an equivalent short-length passive fiber with the same group velocity dispersion (GVD) and negligible nonlinearity, ignoring higher order dispersion contributions and

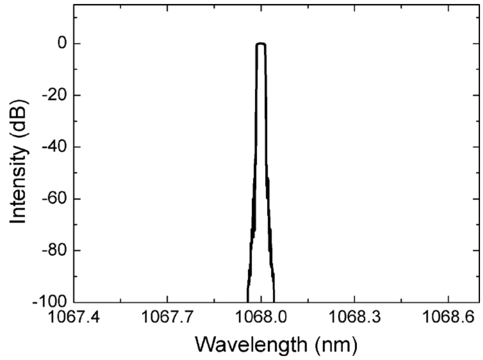

Fig. 5. Simulated spectrum, with a 0.03-nm FWHM bandwidth.

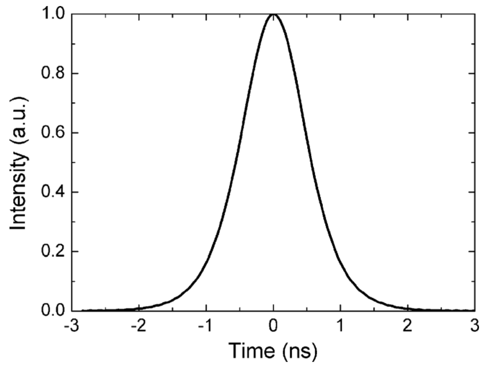

Fig. 6. Simulated temporal intensity profile, with an FWHM duration of 1.15 ns.

with a Gaussian filter with a bandwidth equal to the pass-band of the grating. The simulated temporal and spectral profiles (Figs. 5 and 6) are in good agreement with experimental results for similar intracavity energies: 65 pJ and 60 pJ (taken straight after the OC) for simulation and experiment respectively. The experimental spectrum was recorded on a broader span to show the contribution from the ASE, and thus because of the limited resolution of the diagnostics the square shape to the spectral profile is not evident. However, there is excellent qualitative and quantitative agreement between the experimental and numerical spectra – in particular this is evidenced by the close agreement between the FWHM values.

Control of the intracavity pulse evolution in ANDi lasers can be reduced to three key parameters [13]: the nonlinear phase shift ($\Phi_{\rm NL}$), the effective spectral filtering bandwidth and the GVD. The dominant contribution to the spectral filtering and the GVD is provided by the CFBG; for observed peak powers during stable mode-locking the round-trip $\Phi_{\rm NL} \ll \pi$, explaining the narrow bandwidth spectrum.

A negligible value of $\Phi_{\rm NL}$ can be explained by the low intracavity average power caused by the low saturation power ($\sim$ 6 W) and low damage threshold of the saturable absorber device. Stable operation of the experimental system and convergence of simulations to well matched parameters confirm that nanosecond pulses can be generated in a normally dispersive mode-locked laser using linear dispersion alone, provided by a chirped grating element.

IV. Conclusion

We have demonstrated an ANDi ytterbium-doped all-fiber laser mode-locked by a SWNT saturable absorber generating nanosecond pulses with a large lumped, rather than distributed normal dispersion.

Acknowledgment

The authors would like to thank Dr. J. C. Travers for useful discussions, in particular with regard to numerical aspects.

References

[1] A. Chong, J. Buckley, W. Renninger, and F. Wise, “All-normal-dispersion femtosecond fiber laser,” *Opt. Express*, vol. 14, pp. 10095–10100, 2006.

[2] C. J. S. de Matos, S. V. Popov, A. B. Rulkov, J. R. Taylor, J. Broeng, T. P. Hansen, and V. P. Gapontsev, “All-fiber format compression of frequency chirped pulses in air-guiding photonic crystal fibers,” *Phys. Rev. Lett.*, vol. 93, no. 10, p. 103901, Sep. 2004.

[3] A. B. Rulkov, M. Y. Vyatkin, S. V. Popov, J. R. Taylor, and V. P. Gapontsev, “High brightness picosecond all-fiber generation in 525–1800 nm range with picosecond Yb pumping,” *Opt. Express*, vol. 13, no. 2, pp. 377–381, Jan. 2005.

[4] S. Lefrançois, K. Kieu, Y. Deng, J. D. Kafka, and F. W. Wise, “Scaling of dissipative soliton fiber lasers to megawatt peak power by use of large-area photonic crystal fiber,” *Opt. Lett.*, vol. 35, no. 10, pp. 1569–1571, May 2010.

[5] S. Kobtsev, S. Kukarin, and Y. Fedotov, “Ultra-low repetition rate mode-locked fiber laser with high-energy pulses,” *Opt. Express*, vol. 16, no. 26, pp. 21936–21941, Dec. 2008.

[6] W. H. Renninger, A. Chong, and F. W. Wise, “Dissipative solitons in normal-dispersion fiber lasers,” *Phys. Rev. A*, vol. 77, p. 023814, Feb. 2008.

[7] E. J. R. Kelleher, J. C. Travers, E. P. Ippen, Z. Sun, A. C. Ferrari, S. V. Popov, and J. R. Taylor, “Generation and direct measurement of giant chirp in a passively mode-locked laser,” *Opt. Lett.*, vol. 34, no. 22, pp. 3526–3528, Nov. 2009.

[8] E. J. R. Kelleher, J. C. Travers, Z. Sun, A. G. Rozhin, A. C. Ferrari, S. V. Popov, and J. R. Taylor, “Nanosecond-pulse fiber lasers mode-locked with nanotubes,” *Appl. Phys. Lett.*, vol. 95, p. 111108, Sep. 2009.

[9] A. I. Chernov, E. D. Obraztsova, and A. S. Lobach, “Optical properties of polymer films with embedded single-wall carbon nanotubes,” *Physica Status Solidi B, Basic Solid State Physics*, vol. 244, pp. 4231–4235, Nov. 2007.

[10] E. D. Obraztsova, J. -M. Bonard, V. L. Kuznetsov, V. I. Zaikovskii, S. M. Pimenov, A. S. Pozharov, S. V. Terekhov, V. I. Konov, A. N. Obraztsov, and A. P. Volkov, “Structural measurements for single-wall carbon nanotubes by Raman scattering technique,” *Nanostructured Mater.*, vol. 12, pp. 567–572, 1999.

[11] J. C. Travers, J. Morgenweg, E. D. Obraztsova, A. I. Chernov, E. J. R. Kelleher, and S. V. Popov, “Using the E_{22} transition of carbon nanotubes for fiber laser mode-locking,” *Laser Phys. Lett.*, vol. 8, no. 2, pp. 144–149, 2011.

[12] H. A. Haus, J. G. Fujimoto, and E. P. Ippen, “Structures for additive pulse mode locking,” *J. Opt. Soc. Amer. B*, vol. 8, no. 10, pp. 2068–2076, Oct. 1991.

[13] A. Chong, W. H. Renninger, and F. W. Wise, “Properties of normal-dispersion femtosecond fiber lasers,” *J. Opt. Soc. Amer. B*, vol. 25, no. 2, pp. 140–148, Feb. 2008.